Strongly Correlated Bosons on a Dynamical Lattice

Daniel González-Cuadra,[1] Przemysław R. Grzybowski,[1,2] Alexandre Dauphin,[1] and Maciej Lewenstein[1,3]
[1]ICFO-Institut de Ciències Fotòniques, The Barcelona Institute of Science and Technology, Av. Carl Friedrich Gauss 3, 08860 Barcelona, Spain
[2]Faculty of Physics, Adam Mickiewicz University, Umultowska 85, 61-614 Poznań, Poland
[3]ICREA, Passeig Lluís Companys 23, 08010 Barcelona, Spain

(Received 23 February 2018; published 30 August 2018)

We study a one-dimensional system of strongly correlated bosons on a dynamical lattice. To this end, we extend the standard Bose-Hubbard Hamiltonian to include extra degrees of freedom on the bonds of the lattice. We show that this minimal model exhibits phenomena reminiscent of fermion-phonon models. In particular, we discover a bosonic analog of the Peierls transition, where the translational symmetry of the underlying lattice is spontaneously broken. This provides a dynamical mechanism to obtain a topological insulator in the presence of interactions, analogous to the Su-Schrieffer-Heeger model for electrons. We characterize the phase diagram numerically, showing different types of bond order waves and topological solitons. Finally, we study the possibility of implementing the model using atomic systems.

DOI: 10.1103/PhysRevLett.121.090402

Introduction.—The study of interactions between particles and lattice degrees of freedom (d.o.f.) is of central importance in quantum many-body physics. The interplay between electrons and phonons has been extensively studied, leading to the description of paradigmatic effects such as superconductivity, polaron formation or charge density waves [1,2]. The analogous problem for bosons, on the other hand, has not been extensively investigated. The basic feature of phononic systems is that the lattice may fluctuate or order at various wavelengths. In one dimension, a system of itinerant particles on a deformable lattice can undergo a Peierls transition [3], characterized by the spontaneous breaking of the lattice translational symmetry in a density-dependent manner. For fermions, the statistical correlations induced by Pauli's exclusion principle are sufficient to drive this effect, associated with a gap opening around the Fermi surface. The latter is absent in the bosonic case. However, similar effects still appear in the presence of sufficiently strong interactions, as we report in this Letter.

The study of boson-lattice problems becomes very relevant in the context of quantum simulators. These are versatile platforms where model Hamiltonians can be engineered with an unprecedented degree of control [4,5]. Ultracold atoms in optical lattices, in particular, allow one to experimentally address systems of strongly correlated bosons and to study their properties [6–9], e.g., the realization of the phase transition between a Mott insulator and a superfluid [10] in the Bose-Hubbard model [11]. Since then, a variety of models have been studied—including, e.g., different types of interactions [12,13] or artificial gauge fields [14,15]. These provide an interesting platform to study novel phenomena, such as supersolid phases [16] or topological order [17].

The simulation of these models rely on the implementation of static optical lattices. The particles do not influence the lattice structure and, therefore, phonons are usually not taken into account. Trapped ion systems can also simulate many-body Hamiltonians [18–20]. In these systems, phonons appear naturally [21], and can be used to mediate interactions between the ions [22]. However, trapped ions are confined at the lattice sites, making the simulation of itinerant particles more challenging. Recently, advances in designing systems formed by both neutral atoms and ions [23–30] suggest the possibility of simulating itinerant particles and dynamical lattices simultaneously. This strategy was explored for a chain of fermionic atoms, where a Peierls transition was predicted [24]. Alternative approaches include the use of molecules in self-assembled dipolar lattices [31], optical cavities [32–37], or trapped nanoparticles [38].

In this Letter, we propose and analyze a one-dimensional model of interacting bosons coupled to a dynamical lattice, i.e., deformable and nonadiabatic. We also discuss a possible experimental scheme with ultracold atoms. The most important result is the discovery of bosonic analogs of the Peierls transition, leading to commensurate and incommensurate bond order waves (BOW). For density $\rho = 1/2$, in particular, the ground state corresponds to a dynamically generated topological insulator, supporting edge states and topological solitons, similar to the fermionic SSH model [39]. The proposed model provides a unique playground to study the interplay between strong interactions, lattice dynamics, spontaneous symmetry breaking, and topological effects.

Model.—We introduce a minimal model of strongly correlated bosons interacting with lattice d.o.f. described by a set of independent two-level systems. The Hamiltonian reads

$$\hat{H} = -t\sum_i (\hat{b}_i^\dagger \hat{b}_{i+1} + \text{H.c.}) + \frac{U}{2}\sum_i \hat{n}_i(\hat{n}_i - 1) - \mu\sum_i \hat{n}_i - \alpha\sum_i (\hat{b}_i^\dagger \hat{\sigma}_i^z \hat{b}_{i+1} + \text{H.c.}) + \frac{\Delta}{2}\sum_i \hat{\sigma}_i^z + \beta\sum_i \hat{\sigma}_i^x, \quad (1)$$

where $\hat{b}_i^\dagger$ creates a boson on site i and $\hat{n}_i = \hat{b}_i^\dagger \hat{b}_i$ is the number operator. $\hat{\sigma}_i^z$ and $\hat{\sigma}_i^x$ are Pauli operators associated with a spin-1/2 system living on the bond between sites i and $i+1$. The first three terms of Eq. (1) correspond to the standard Bose-Hubbard Hamiltonian [11]. The next term describes a lattice-dependent boson tunneling. The total hopping through a bond is maximized (minimized) for a spin in the "up" ("down") state. Finally, the last two terms introduce the spin dynamics. The Hamiltonian (1) bears similarities with models with spin dependent hoppings, such as quantum link models [40].

In this work, we focus on the regime of quasiadiabatic spins ($\beta \ll t$). In this limit, the ground state of the spins depends on the competition between two terms: the energy difference Δ and the interaction α with the bosons. If one dominates, the expectation value $\langle \hat{\sigma}_i^z \rangle$ will be uniform and close to -1 ($\Delta \gg \alpha$) or $+1$ ($\Delta \ll \alpha$). When the two are comparable, phases with broken translational symmetry arise.

Hardcore bosons.—Consider an adiabatic lattice, $\beta = 0$, in the hardcore boson limit, $U \to \infty$. After a Jordan-Wigner transformation, the model is mapped to a system of spinless fermions in a classical background. At half filling, the spin configuration minimizing energy is staggered (Néel order) for values of Δ between two critical points, $\Delta_c^\pm = (4t/\pi)[\delta \pm (E(1-\delta^2) - 1)]$, where $\delta = \alpha/t$ and $E(x)$ is a complete elliptic integral of the second kind [41]. From the fermions' viewpoint, this leads to the development of a staggered order on the bonds, a gap opens at the Fermi surface, and the system becomes insulating. This effect appears when the lattice deformation, which breaks translational invariance, has a wavelength equal to π/k_F, where k_F is the Fermi wave vector. This is the mechanism behind the Peierls instability [3]. Thus, our minimal model is capable of describing analogous phenomena such as those appearing in more complicated fermion-lattice systems [39].

Finite interactions.—For finite values of U, we enter into the strongly correlated boson regime, and the mapping to noninteracting fermions is not possible. To calculate the ground state of the system, we use a DMRG algorithm with bond dimension $D = 40$ [45]. We consider a system size of $L = 60$ sites (and $L-1$ bonds), and work with open boundary conditions. We truncate the maximum number of bosons per site to $n_0 = 2$. This approximation is justified for low densities and strong interactions [41]. In the following, we fix the values of the parameters to $t = 1$, $\alpha = 0.5$, and $\beta = 0.02$.

At the bosonic density $\rho = 1/2$, the Neel order survives for finite values of U, and disappears for small interactions. Strong correlations are needed, therefore, to have a bosonic Peierls phase. The Bose-Hubbard model on a fixed bond-dimerized lattice was previously studied, revealing an insulating phase at $\rho = 1/2$ [46], and the presence of topological edge states [47]. Here, the same superlattice structure is obtained dynamically, in the spirit of the original SSH model for fermions and phonons [39]. We also observe edge states which will be studied in a separate work [48]. We focus here on a different topological effect also present in the SSH model: the solitonic solutions. These are a consequence of the double degenerate ground state at $\rho = 1/2$, corresponding to the two inverted staggered patterns, and only occur when quantum fluctuations on the lattice are present.

For $U = 10$, we study the phase diagram of the model in terms of Δ and ρ. For $\Delta \gg \alpha$ or $\Delta \ll \alpha$, the spin configuration in the ground state is uniform. The bosonic part of the Hamiltonian (1) is qualitatively similar to the Bose-Hubbard model [11], with a Mott insulator (MI) and a superfluid phase (SF). In an intermediate regime ($\Delta \approx 0.6$–1.0), the translational symmetry is broken in the ground state for a substantial range of densities. Figure 1 shows the spatial structure on the bonds (a) and sites (b) for $\Delta = 0.85$. For $\rho = 1/2$ and $2/3$, the unit cell is enlarged to two and three sites, respectively. Similarly to $\rho = 2/3$, a trimer configuration appears for $\rho = 1/3$ at a different Δ. For densities close to the mentioned ones, long wavelength modulations appear on top of the corresponding patterns. These are solitonic configurations where the underlying order—staggered in

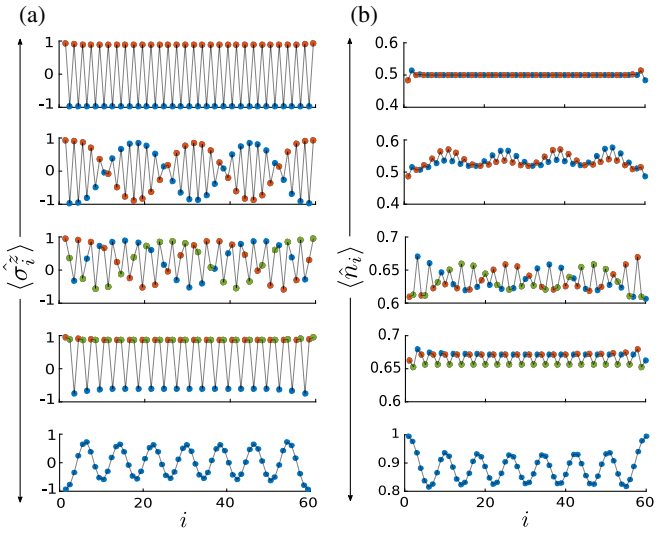

FIG. 1. Spatial structure of bond (a) and site (b) expectation values for $\Delta = 0.85$ and different bosonic densities, showing some of the representative orders that can develop. From above to below: $\rho = 1/2$, $\rho = 1/2 + 2/60$, $\rho = 2/3 - 2/60$, $\rho = 2/3$, and $\rho = 0.88$. Different colors represent different sublattice elements, making explicit the long-wavelength modulations on top of the underlying order.

the half-filled case—is reversed periodically forming kinks; the "extra" bosons or holes lead to increased density modulations, located around the kinks [2nd or 3rd row in panel (b)]. Finally, close to $\rho = 1$, long wavelength structures appear. The bosonic hopping $\langle \hat{b}_i^\dagger \hat{b}_{i+1} + \text{H.c.} \rangle$ presents the same spatial pattern as $\langle \hat{\sigma}_i^z \rangle$ in all the cases. We therefore focus on the latter quantity for simplicity. The ground states, shown in Fig. 1, possess long-range order. We refer to the corresponding quantum phases as bond order waves, since the bosonic order is block diagonal. In many cases, this bond order is accompanied by small density waves. We consider the spin structure factor

$$S_\sigma(k) = \frac{1}{L^2} \sum_{i,j} e^{(x_i - x_j)ki} \langle (\hat{\sigma}_i^z - \bar{\sigma^z})(\hat{\sigma}_j^z - \bar{\sigma^z}) \rangle, \qquad (2)$$

with $\bar{\sigma}^z = \sum_i \langle \hat{\sigma}_i \rangle / L$, where the summations run over all bonds. This quantity develops a peak for some k_0 in the presence of long-range order, and its height can be used as an order parameter. Figure 2 shows $S_\sigma^{\max}$ in terms of Δ for $\rho = 0.733$, which qualitatively distinguishes a uniform SF phases from a solitonic BOW. The inset (a) presents S_σ for $\Delta = 0.90$, where a peak develops for $k_0 = 8\pi/15$. From this wave vector, an order wavelength can be defined as $\lambda_0 = 2\pi/k_0$. We note that, in this case, λ_0 is not an integer factor of the lattice spacing a (fixed to one here). This is also the case for the other solitonic and long-wavelength BOW phases. We refer to these orders as *incommensurate* (iBOW). For $\rho = 1/3, 1/2$, and $2/3$, however, S_σ presents a peak at $\pi/3$, π, and $2\pi/3$, respectively, with wavelengths of the form $a\mathbb{N}$. We call the latter *commensurate* orders (cBOW). While a long-range order is expected in commensurate phases, its presence in incommensurate ones (especially solitonic) is a special feature of the model, related to the Peierls instability. The inset (b) shows the scaling of $S_\sigma(k)$ with the system size, for $k = k_0$ and $k = \pi$ and for two representative incommensurate cases: $\rho = 0.55$ (solitonic) and $\rho = 0.85$ (long-wavelength). The fit, containing terms up to $O(1/L^3)$, shows that the long-range order exists in the thermodynamic limit.

One of the principal features of the theory of Peierls transition is the relation between the order wave vector and the Fermi wave vector [3]. In one-dimensional systems with a two-point Fermi surface, the theory predicts $k_0 = 2k_F = 2\rho\pi$, independently of the fermion dispersion and the form of the fermion-lattice interaction. Remarkably, we found the same relation for bosonic Peierls transitions [inset (b) of Fig. 3], where the Fermi surface is absent. This relation holds in the presence of next neighbor hopping $-t' \sum_i (\hat{b}_i^\dagger \hat{b}_{i+2} + \text{H.c.})$, where even hard-core bosons cannot be mapped onto fermions [49]. This suggests that Peierls transitions require a deeper theory unifying the fermionic and bosonic cases.

There are no off-diagonal bosonic long-range orders coexisting with the BOW order. We found superfluid, on-site pair superfluid and intersite pair superfluid correlations to decay exponentially in the BOW phases [41]. Additionally, the scaling of the entanglement entropy shows that all BOW phases are gapped, although in the case of iBOW phases the gap is probably quite small [41]. Therefore, the solitonic phases present in our model are qualitatively different from those appearing in the extended Bose-Hubbard model [50].

Interestingly, the iBOW phases are compressible, with compressibility $\kappa = \partial\rho/\partial\mu \neq 0$. This is in contrast to the behavior of many bosonic models, where the presence of a gap and a diagonal or block-diagonal order usually implies incompressibility. Figure 3 depicts the density ρ in terms of μ for $\Delta = 0.87$. Here, a superfluid phase occurs for

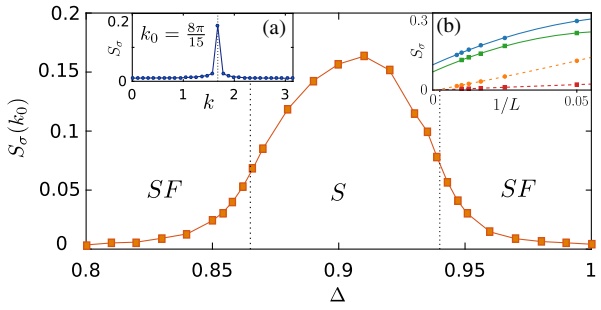

FIG. 2. Structure factor at k_0 in terms of Δ. It allows one to qualitatively distinguish between the iBOW and the uniform SF phases. The exact location of the critical points (dotted lines) is found through a finite-size scaling of the fidelity susceptibility [41]. Inset: (a) Structure factor $S(k)$ in the solitonic phase (S), for $\rho = 0.733$ and $\Delta = 0.90$. A clear peak is observed at $k_0 = 8\pi/15$. (b) Finite-size scaling of $S_\sigma(k)$ for $\rho = 0.55$ (circles) and $\rho = 0.85$ (squares), for $k = k_0(\rho)$ (continuous line) and $k = \pi$ (dashed line).

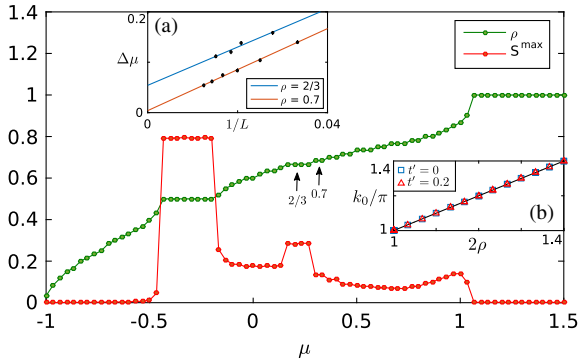

FIG. 3. Density ρ and maximum structure factor $S^{\max}$ in terms of the chemical potential μ for $\Delta = 0.87$ and $L = 60$. The structure factor has nonzero values for the BOW phases. Plateaus in the density are related to incompressible phases, but they can also appear as finite size effects. Insets: (a) Scaling of the plateaus $\Delta\mu$ for different system sizes for a cBOW phase ($\rho = 2/3$) and for a solitonic iBOW one ($\rho = 0.7$) (b) k_0 vs ρ for $t' = 0$ and $t' = 0.2$ (see main text).

$0 < \rho < 1/2$, and BOW phases appear for $1/2 \leq \rho < 1$. Finally, $\rho = 1$ corresponds to a MI. The plateaus in the $\mu - \rho$ line signal the incompressible phases, which, apart from the MI, correspond to a cBOW phase at $\rho = 1/2$ and $\rho = 2/3$. The finite size scaling of other plateaus [inset (a)] reveals that the iBOW phases are indeed compressible.

In the hardcore limit, the presence of a gap, together with a long-range order, and a nonzero compressibility can be understood using the single-particle fermionic picture. For increasing particle density, the added particles will not occupy states above the gap. The $k_0 = 2k_F = 2\rho\pi$ relation means that the position of the gap will be adjusted to the new Fermi level. The composite spin-particle system avoids the gap penalty by the modification of the effective lattice structure. For strongly correlated bosons the mechanism is more complicated, as the Fermi energy picture is lacking. However, many of the properties remain. In particular, the relation $k_0 = 2k_F = 2\rho\pi$ still holds. Therefore, neither the presence of a gap nor long-range order necessarily exclude compressibility. Nonetheless, the commensurate orders are incompressible (cBOW). This implies that these orders are more stable under small changes of the chemical potential. Figure 3 shows the maximum value of the structure factor ($S_\sigma^{\max}$) as a function of μ. It is zero for the uniform phases (MI and SF) and it changes continuously among the BOW phases, except for the commensurate orders where it clearly stands out. Since $S_\sigma^{\max}$ represents an order parameter, this behavior corresponds to finite changes in the free energy as the density is varied, meaning that these *pinned* wavelengths are energetically more stable.

For a wide range of values of Δ, we calculate the plateau size and the maximum structure factor in terms of μ. These two properties are sufficient to identify all the phases of the model. The results are summarized in the phase diagram (Fig. 4). Inside the MI, the spins are uniform and $\langle \hat{\sigma}_i^z \rangle$ changes continuously from $+1$ to -1 as Δ increases. As a consequence, the boundary between this phase and the SF is modified. The phase diagram also shows the extensions of the BOW phases, the most stable one being $\mathrm{cBOW}_{1/2}$.

Experimental implementation.—To realize the proposed model (1), we consider first a gas of ultracold bosonic atoms in an optical lattice, described by the Bose-Hubbard Hamiltonian. A second optical lattice, trapping either neutral or charged atoms, is introduced, placing its minima between two minima of the first lattice. The atoms corresponding to the second lattice have two internal d.o.f.—representing spin systems—and the potential is deep enough to confine them [41]. As shown in Refs. [23,25,51,52], in this situation, the hopping of the moving particles between two neighboring sites is influenced by the internal state of the corresponding spin, giving rise to the desired boson-spin interaction. The on-site boson interaction term can be influenced by the internal state of the spins. However, this dependence is very weak [25], and we neglect it here. The spin part of the Hamiltonian can be implemented as follows: the energy difference between the two spin states is obtained by introducing an external magnetic field, and the spin flipping is enforced using laser-assisted transitions between the two states. This strategy is valid both when the impurity corresponds to a neutral atom or to an ion. Although the boson-spin interaction α might be difficult to tune in an experiment, the phases we show in this work are present for a broad range of values of this parameter, for a suitably chosen Δ. The different phases could be detected by measuring the spin structure factor [53–55] and the compressibility in the atomic system [56,57].

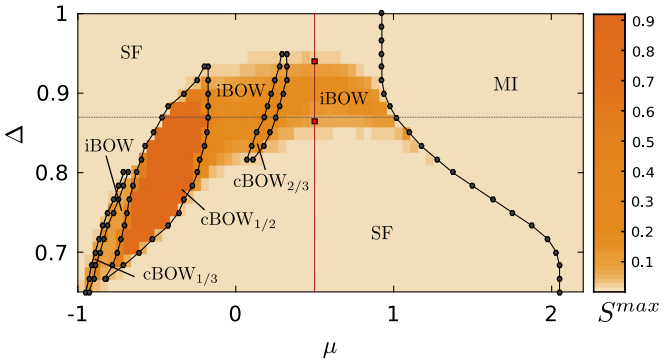

FIG. 4. Phase diagram of the Hamiltonian (1) for a system size of $L = 60$ in terms of Δ and μ. The solid black lines delimit the incompressible phases (cBOW and MI). The maximum value of the structure factor is represented by the color plot, qualitatively distinguishing between the iBOW and SF phases. The dotted lines correspond to the cuts for $\mu = 0.5$ (Fig. 2) and $\Delta = 0.87$ (Fig. 3). For the former, the red squares mark two critical points in the thermodynamic limit.

Summary.—We introduced a boson-spin Hamiltonian that models the behavior of strongly correlated bosons on a dynamical lattice, and demonstrated the possibility of obtaining bosonic analogs of the Peierls phase. We characterized the phases of the system in the quasiadiabatic limit (slow lattice dynamics), using the spin structure factor, entanglement entropy, and compressibility. We found, besides the uniform SF and MI phases, compressible and incompressible bond order waves. We also discussed the possibility of implementing the model using ultracold atoms and ions trapped in optical lattices. In the future, it would be interesting to study more extensively the topological properties of the model, as well as the regime of nonadiabatic spins.

The authors thank A. Celi, R. W. Chhajlany, A. Piga, L. Tarruell, and E. Tirrito for useful discussions. This work has been supported by the Spanish Ministry MINECO (National Plan 15 Grant: FISICATEAMO No. FIS2016-79508-P, SEVERO OCHOA No. SEV-2015-0522, FPI), European Social Fund, Fundació Cellex, Generalitat de Catalunya (AGAUR Grant No. 2017 SGR 1341 and

CERCA/Program), ERC AdG OSYRIS, EU FETPRO QUIC, and the National Science Centre, Poland-Symfonia Grant No. 2016/20/W/ST4/00314. D. G.-C. is financed by the ICFOstepstone–PhD Programme for Early-Stage Researchers in Photonics, funded by the Marie Skłodowska-Curie Co-funding programmes (GA665884) of the European Commission. A. D. is financed by a Cellex-322 ICFO-MPQ fellowship.

[1] A. Altland and B. Simons, *Condensed Matter Field Theory* (Cambridge University Press, Cambridge, England, 2006).
[2] D. Emin, *Polarons* (Cambridge University Press, Cambridge, England, 2012).
[3] R. Peierls, *Quantum Theory of Solids*, International Series of Monographs on Physics (Clarendon Press, Oxford, 1955).
[4] I. Buluta and F. Nori, Science **326**, 108 (2009).
[5] J. I. Cirac and P. Zoller, Nat. Phys. **8**, 264 (2012).
[6] D. Jaksch and P. Zoller, Ann. Phys. (Amsterdam) **315**, 52 (2005).
[7] I. Bloch, J. Dalibard, and W. Zwerger, Rev. Mod. Phys. **80**, 885 (2008).
[8] I. Bloch, Nat. Phys. **1**, 23 (2005).
[9] M. Lewenstein, A. Sanpera, and V. Ahufinger, *Ultracold Atoms in Optical Lattices: Simulating Quantum Many-body Systems* (Oxford University Press, Oxford, 2017).
[10] M. Greiner, O. Mandel, T. Esslinger, T. W. Hänsch, and I. Bloch, Nature (London) **415**, 39 (2002).
[11] M. P. A. Fisher, P. B. Weichman, G. Grinstein, and D. S. Fisher, Phys. Rev. B **40**, 546 (1989).
[12] V. W. Scarola and S. Das Sarma, Phys. Rev. Lett. **95**, 033003 (2005).
[13] O. Dutta, M. Gajda, P. Hauke, M. Lewenstein, D.-S. Lühmann, B. A. Malomed, T. Sowiński, and J. Zakrzewski, Rep. Prog. Phys. **78**, 066001 (2015).
[14] N. Goldman, G. Juzelinas, P. Öhberg, and I. B. Spielman, Rep. Prog. Phys. **77**, 126401 (2014).
[15] J. Dalibard, F. Gerbier, G. Juzeliūnas, and P. Öhberg, Rev. Mod. Phys. **83**, 1523 (2011).
[16] G. G. Batrouni, F. Hébert, and R. T. Scalettar, Phys. Rev. Lett. **97**, 087209 (2006).
[17] E. G. Dalla Torre, E. Berg, and E. Altman, Phys. Rev. Lett. **97**, 260401 (2006).
[18] R. Blatt and C. F. Roos, Nat. Phys. **8**, 277 (2012).
[19] C. Schneider, D. Porras, and T. Schätz, Rep. Prog. Phys. **75**, 024401 (2012).
[20] M. Johanning, A. F. Varn, and C. Wunderlich, J. Phys. B **42**, 154009 (2009).
[21] D. Leibfried, R. Blatt, C. Monroe, and D. Wineland, Rev. Mod. Phys. **75**, 281 (2003).
[22] D. Porras and J. I. Cirac, Phys. Rev. Lett. **92**, 207901 (2004).
[23] A. Negretti, R. Gerritsma, Z. Idziaszek, F. Schmidt-Kaler, and T. Calarco, Phys. Rev. B **90**, 155426 (2014).
[24] U. Bissbort, D. Cocks, A. Negretti, Z. Idziaszek, T. Calarco, F. Schmidt-Kaler, W. Hofstetter, and R. Gerritsma, Phys. Rev. Lett. **111**, 080501 (2013).
[25] R. Gerritsma, A. Negretti, H. Doerk, Z. Idziaszek, T. Calarco, and F. Schmidt-Kaler, Phys. Rev. Lett. **109**, 080402 (2012).
[26] J. Joger, A. Negretti, and R. Gerritsma, Phys. Rev. A **89**, 063621 (2014).
[27] A. Härter and J. H. Denschlag, Contemp. Phys. **55**, 33 (2014).
[28] A. T. Grier, M. Cetina, F. Oručević, and V. Vuletić, Phys. Rev. Lett. **102**, 223201 (2009).
[29] C. Zipkes, S. Palzer, C. Sias, and M. Köhl, Nature (London) **464**, 388 (2010).
[30] S. Schmid, A. Härter, and J. H. Denschlag, Phys. Rev. Lett. **105**, 133202 (2010).
[31] G. Pupillo, A. Griessner, A. Micheli, M. Ortner, D.-W. Wang, and P. Zoller, Phys. Rev. Lett. **100**, 050402 (2008).
[32] I. B. Mekhov, C. Maschler, and H. Ritsch, Nat. Phys. **3**, 319 (2007).
[33] J. Larson, B. Damski, G. Morigi, and M. Lewenstein, Phys. Rev. Lett. **100**, 050401 (2008).
[34] K. Baumann, C. Guerlin, F. Brennecke, and T. Esslinger, Nature (London) **464**, 1301 (2010).
[35] F. Piazza and P. Strack, Phys. Rev. Lett. **112**, 143003 (2014).
[36] R. Landig, L. Hruby, N. Dogra, M. Landini, R. Mottl, T. Donner, and T. Esslinger, Nature (London) **532**, 476 (2016).
[37] F. Mivehvar, H. Ritsch, and F. Piazza, Phys. Rev. Lett. **118**, 073602 (2017).
[38] M. Gullans, T. G. Tiecke, D. E. Chang, J. Feist, J. D. Thompson, J. I. Cirac, P. Zoller, and M. D. Lukin, Phys. Rev. Lett. **109**, 235309 (2012).
[39] A. J. Heeger, S. Kivelson, J. R. Schrieffer, and W. P. Su, Rev. Mod. Phys. **60**, 781 (1988).
[40] U.-J. Wiese, Ann. Phys. (Amsterdam) **525**, 777 (2013).
[41] See Supplemental Material at http://link.aps.org/supplemental/10.1103/PhysRevLett.121.090402 for further details on the ground state properties of the model in the hardcore limit, the properties of the BOW phases, the numerical method used, and the experimental realization, which includes Refs. [42–44].
[42] P. Calabrese and J. Cardy, J. Stat. Mech. Theory Exp. **2004**, P06002 (2004).
[43] J. Eisert, M. Cramer, and M. B. Plenio, Rev. Mod. Phys. **82**, 277 (2010).
[44] S.-J. Gu, Int. J. Mod. Phys. B **24**, 4371 (2010).
[45] U. Schollwöck, Ann. Phys. (Amsterdam) **326**, 96 (2011).
[46] P. Buonsante, V. Penna, and A. Vezzani, Phys. Rev. A **70**, 061603 (2004).
[47] F. Grusdt, M. Höning, and M. Fleischhauer, Phys. Rev. Lett. **110**, 260405 (2013).
[48] D. González-Cuadra, P. R. Grzybowski, A. Dauphin, and M. Lewenstein (unpublished).
[49] We note that the presence of next-nearest neighbor hopping terms changes the topology of the systems from a chain into a zigzag ladder, which raises the question about similar results in two-dimensional systems.
[50] T. Mishra, R. V. Pai, S. Ramanan, M. S. Luthra, and B. P. Das, Phys. Rev. A **80**, 043614 (2009).

[51] A. Micheli, A. J. Daley, D. Jaksch, and P. Zoller, Phys. Rev. Lett. **93**, 140408 (2004).
[52] J. M. Schurer, R. Gerritsma, P. Schmelcher, and A. Negretti, Phys. Rev. A **93**, 063602 (2016).
[53] R. A. Hart, P. M. Duarte, T.-L. Yang, X. Liu, T. Paiva, E. Khatami, R. T. Scalettar, N. Trivedi, D. A. Huse, and R. G. Hulet, Nature (London) **519**, 211 (2015).
[54] M. F. Parsons, A. Mazurenko, C. S. Chiu, G. Ji, D. Greif, and M. Greiner, Science **353**, 1253 (2016).
[55] A. Mazurenko, C. S. Chiu, G. Ji, M. F. Parsons, M. Kanász-Nagy, R. Schmidt, F. Grusdt, E. Demler, D. Greif, and M. Greiner, Nature (London) **545**, 462 (2017).
[56] U. Schneider, L. Hackermüller, S. Will, T. Best, I. Bloch, T. A. Costi, R. W. Helmes, D. Rasch, and A. Rosch, Science **322**, 1520 (2008).
[57] V. W. Scarola, L. Pollet, J. Oitmaa, and M. Troyer, Phys. Rev. Lett. **102**, 135302 (2009).